Discriminating time-varying loads and rotor cage fault in Induction motors

A. E. Mabrouk, S. E. Zouzou, M. Sahraoui and S. Khelif

Abstract -- **Diagnosis of electrical machines are becoming more and more important issues in the field of electrical machines as new data processing technique. Motor Current Stator Analysis (MCSA) are usually used to detect the broken bars. In several industrial applications, the motor is subjected to load torque variations of low frequencies, which have effects similar to rotor faults in the current spectrum and result of diagnostic procedure may be ambigues. Discriminating rotor cage fault from oscillating load effects in Induction motors must be considered.**

In this paper, we present a study based on the application of the active and reactive power signature analyses for discriminating broken rotor bars from mechanical load oscillation effects in operating three-phase squirrel cage induction motors. This method is attractive because it does not need to interrupt the operating system. Finite element method was used to perform dynamical simulation, which leads to more precise results than other models, as the reel geometry and winding layout of the machine are used. The computer simulations and laboratory experiments results show the interest and the efficiency of this technique for the correct distinction between broken rotor bars and load oscillations.

Index Terms-- Squirrel cage induction motor, instantaneous active power, instantaneous reactive power, broken bar, finite element analysis, load oscillation.

I. INTRODUCTION

Nowadays three-phase induction motors are used in a wide variety of industrial applications. They are the most used kind of electrical machines. However, electrical and mechanical faults pose a particular challenge to the industry and end users which often interrupt the productivity and require maintenance. In literature, rotor faults have been shown to account for a large portion of induction motor failures, sometimes they are the single biggest cause of failure in the field. Under the assumption of a constant load torque, Motor Current Stator Analysis (MCSA) are usually used to detect the broken bars [1]-[2]. The corresponding side-band characteristic harmonics are located at:

$$f_b = (1 \pm 2ks) f_s \tag{1}$$

Where f_s is the electrical supply frequency and s is the rotor slip.

In several industrial applications, like cement industry, the motor is subjected to load torque variations of low frequencies, due to cyclic variations of the industrial process. Considering only the fundamental component in the Fourier series development, the load torque is described by:

$$T_{load}(t) = T_{avg} + T_{osc} \cos(2\pi f_0 t) \tag{2}$$

Where T_{load} is the torque load, T_{avg} is the average load, T_{osc} is oscillated part of torque, f_0 is the load torque frequency. If f_0 is similar to $2sf_s$, the same spectral components mentioned in (1) can be found in the motor current spectrum even when the motor is in healthy conditions [3]. In this case, the commonly used MCSA does not allow discriminating between a motor with broken rotor bars from a motor driven by an oscillating load. Several research works addressing this problem have been published, extended Park's vector approach [4], detecting negative sequence harmonics information [5], model reference estimation [3], time-frequency approach [6], Vienna monitoring methods [7], neural networks [8], current space vector [9], Instantaneous Active and Reactive Currents [10] and in recently publications, different powers and their derived quantities [11]-[13].

In this paper, the instantaneous active and reactive powers spectra are used to distinguish between broken rotor bars and square-wave torque effect. This analysis is validated through the use of a FEM model and laboratory experiments.

.

II. ACTIVE AND REACTIVE POWERS ANALYSES

The instantaneous active power $p_0(t)$ and reactive power $q_0(t)$ in the healthy case are [11]:

$$p_0(t) = v_a i_a + v_b i_b + v_c i_c = 3VI\cos(\varphi) \tag{3}$$

$$q_0(t) = \sqrt{3}(v_a i_b + v_b i_a) = 3VI\sin(\varphi) \tag{4}$$

The spectra of the instantaneous active and reactive powers contain only a dc component corresponding to their mean values. The rotor cage fault or mechanical abnormality is characterized by the appearance of a sequence of sideband components around the fundamental [11]-[14]:

A. E. Mabrouk, S. E. Zouzou, M. Sahraoui and S. Khelif are with Laboratoire LGEB, Université de Biskra, 07000 Biskra, Algérie (e-mail: h_mabrouk@rocketmail.com). (e-mail: zouzou_s@hotmail.com). (e-mail: s_moh78@yahoo.fr).(khelifsamia@gmail.com)

978-1-4799-0025-1/13/$31.00 ©2013 IEEE

$$i_a(t) = i_f \cos(\omega_s t - \alpha_0) + \sum_{k=1}^{\infty}\{ I_{dl,k} \cos[(1-2ks)\omega_s t - \beta_{l,k}] + \sum_{k=1}^{\infty} I_{dr,k} \cos[(1+2ks)\omega_s t - \beta_{r,k}]\} \quad (5)$$

$$i_b(t) = i_f \cos(\omega_s t - \alpha_0 - 2\pi/3) + \sum_{k=1}^{\infty}\{ I_{dl,k} \cos[(1-2ks)\omega_s t - \beta_{l,k} - 2\pi/3] + \sum_{k=1}^{\infty} I_{dr,k} \cos[(1+2s)\omega_s t - \beta_{r,k} - 2\pi/3]\} \quad (6)$$

$$i_c(t) = i_f \cos(\omega_s t - \alpha_0 + 2\pi/3) + \sum_{k=1}^{\infty}\{ I_{dl,k} \cos[(1-2ks)\omega_s t - \beta_{l,k} + 2\pi/3] + \sum_{k=1}^{\infty} I_{dr,k} \cos[(1+2s)\omega_s t - \beta_{r,k} + 2\pi/3]\} \quad (7)$$

Where:

i_f : maximum value of the fundamental of phase current (A);
α_0 : initial phase angle of the fundamental current;
$i_{dl,k}$: maximum value of the current lower sideband component, at a frequency of $(1\text{-}2ks)f_s$ (A);
$\beta_{l,k}$: initial phase angle of the current lower sideband component;
$i_{dr,k}$: maximum value of the current upper sideband component, at a frequency of $(1+2ks)f_s$ (A);
$\beta_{r,k}$: initial phase angle of the current upper sideband component.
Similarly, the instantaneous power can be described as:

$$p(t) = 3VI\cos(\varphi) + 3V\{\sum_{k=1}^{\infty}[I_{dl,k}\cos(2ks\omega_s t + \beta_{l,k}) - I_{dr,k}\cos(2ks\omega_s t - \beta_{r,k})]\} \quad (8)$$

$$q(t) = 3VI\sin(\varphi) + 3V\{\sum_{k=1}^{\infty}[I_{dl,k}\sin(2ks\omega_s t + \beta_{l,k}) - I_{dr,k}\sin(2ks\omega_s t - \beta_{r,k})]\} \quad (9)$$

It can be seen that the instantaneous total active and reactive powers become different from the healthy case ones. The additional component at the disturbance frequency $f=2ksf_s$ in their spectra, provide extra diagnostic information about the machine condition in the presence of broken rotor bars or load torque oscillations.

III. Simulation Results

In recent years, Finite Element Method (FEM) was widely used in the design and analysis of electric machines. It was proved that the FEM based analysis is an effective and inexpensive method for studying the influence of the faults on the electrical machine behavior [15]. Several program packages for magnetic field computations have been developed (Flux, Maxwell, Ansys, femm …).
The magnetic circuit of the considered induction motor is shown in Fig. 1. The mesh made on the magnetic circuit is denser in the vicinity of the air gap, where the electromagnetic exchanges between the stator and the rotor are carried out.

The 2D electromagnetic field computation model in (x, y) Cartesian coordinates is based on the magnetic vector potential formulation characterized by the following partial differential equation:

$$\nabla\times(\frac{1}{\mu}\nabla\times\vec{A}) + \sigma(\frac{\partial\vec{A}}{\partial t} - \vec{v}\times(\nabla\times\vec{A})) = \vec{J_s} \quad (10)$$

Where:

μ : Magnetic permeability;
A : Magnetic vector potential;
σ : Electrical conductivity;
v : Velocity;
J_s : Current density.

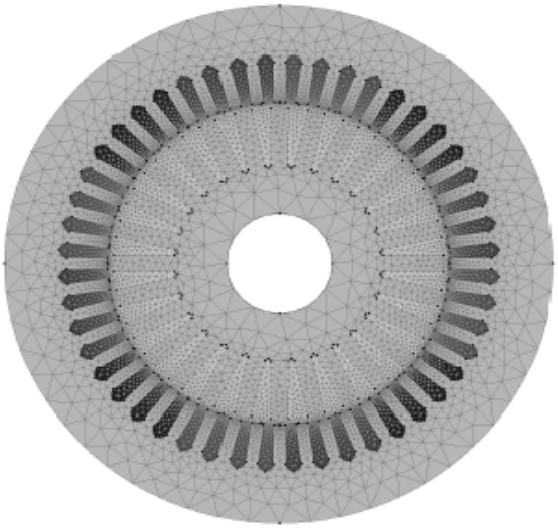

Fig. 1. Geometry and mesh of computation domain.

The use of the rotating air gap, allows considering the rotation of the rotor in the magneto-evolutionary study without making a new mesh of the geometry at each position of the rotor and keeps the same number of unknowns, hence, eliminate the velocity term in (10) [16]. Since the studied induction motor is voltage supplied, the motor is excited to its rated voltage and frequency using a three-phase voltage source, the two unknowns quantities A and J_s in (10) are determined by a field-circuit coupling model of the machine. Once the magnetic field is determined by the time-stepping finite-element method, the magnetic torque is calculated using the Maxwell stress tensor. The mechanical equation determines a new angular and radial position of the. Rotor motion is governed by the mechanical equation:

$$J\ \ddot{w} = T_m - T_l - B\ w \quad (11)$$

Where:

J : is the moment of inertia;

$\ddot{w}$: is the angular acceleration;
w : is the angular velocity;
T_m : is the electromagnetic torque;
T_l: is the torque load;
B : is the friction coefficient.

Hence having the mechanical equations coupled with magnetic equations, the dynamic behavior of the motor can be simulated in any moment.

The characteristics of the induction motor are shown in Table I in appendix.

In our simulation, two cases are simulated: two broken bars, healthy motor with oscillating torque.

Fig. 2 shows the waveform of the torque imposed to the motor. The torque oscillates between two values according to time. In this case, the load torque presents a harmonic components at the frequency f_o=1 Hz similar to $2sf_s$, used to detect the broken bars.

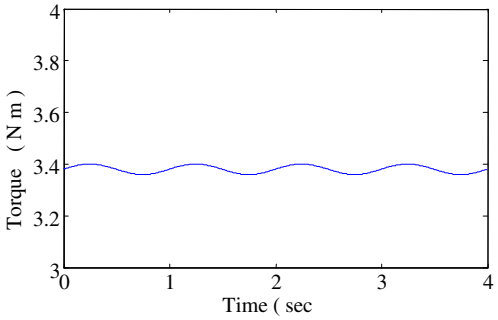

Fig. 2. The shaft torque

Fig. 3 shows the magnetic flux distribution at the transient state for two broken bars and healthy rotor with oscillating torque. When the slip is large, the eddy current shows a large value. This high value of slip is necessary to illustrate the effects of the broken bars on the magnetic field.

The concentration of magnetic flux is observed around the broken bar and creates asymmetric magnetic flux distribution. This is due to the fact that in the broken bar region there is no localized conductor demagnetization effect since these bars carry no currents.

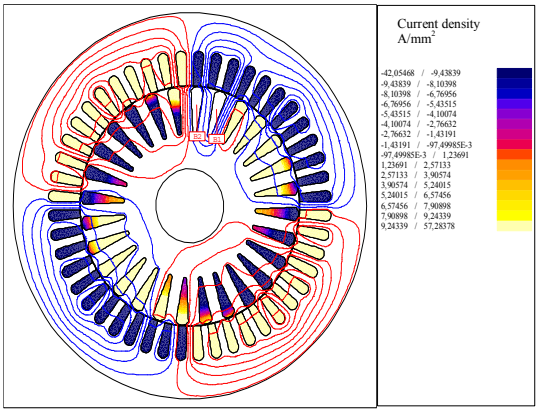

a) Two broken rotor bars

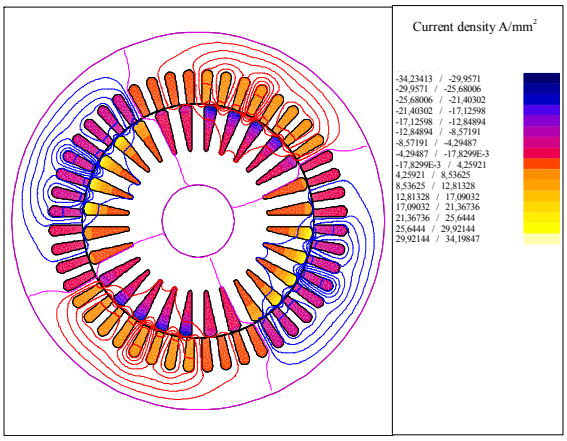

b) Healthy Motor with oscillating torque.

Fig. 3. Magnetic flux and current density at start up.

On Fig. 4, it is obvious that the region around the broken bar of the rotor has a higher degree of saturation compared to the same region in healthy state with oscillating torque. The current densities in the neighbored rotor bars to those broken are significantly increased.

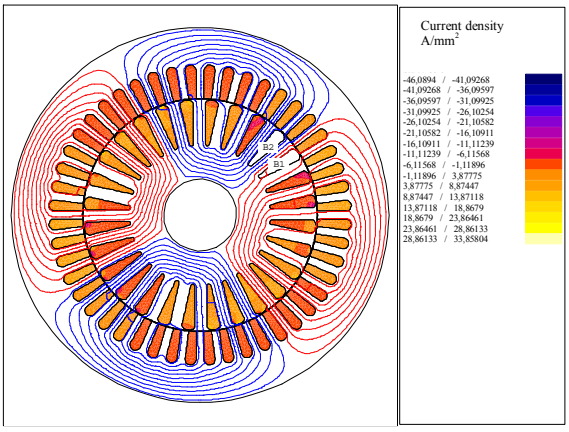

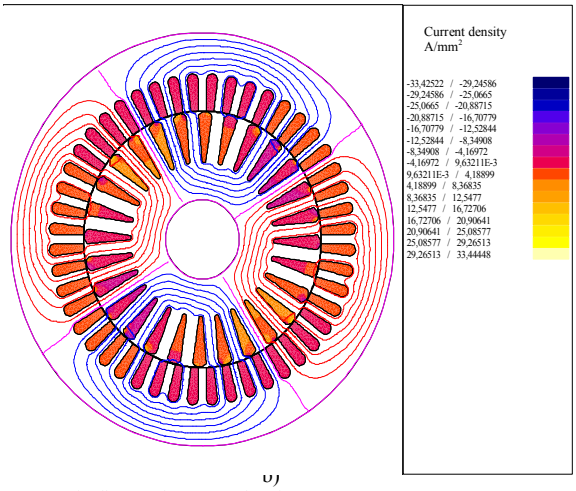

b)

Fig. 4. Magnetic flux and current density at t= 2.297 s.
a) Two broken rotor bars b) Healthy Motor with oscillating torque.

Fig. 5 shows the waveform of the air gap flux density along a circular contour in the air-gap. The flux densities have a symmetrical distribution in healthy state with an oscillating

torque. The perturbation in the magnetic field produced by two broken bars results in a non-symmetrical field.

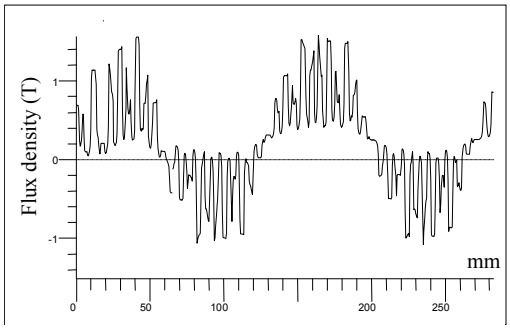

a)

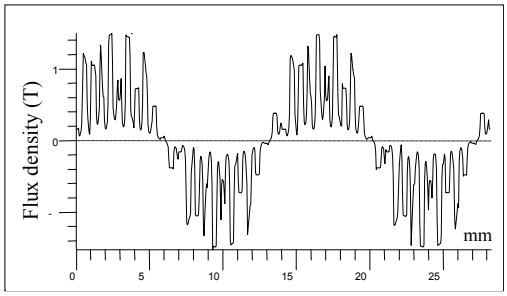

b)

Fig. 5. Waveform of the Air gap flux density at t= 2.297 s.
a) Two broken rotor bars b) Healthy Motor with oscillating torque.

The evolution of the electromagnetic torque and speed, during the first seconds after the connection, for the case of two broken bars and for healthy rotor with load torque oscillation is shown in fig. 6 and fig. 7, respectively.

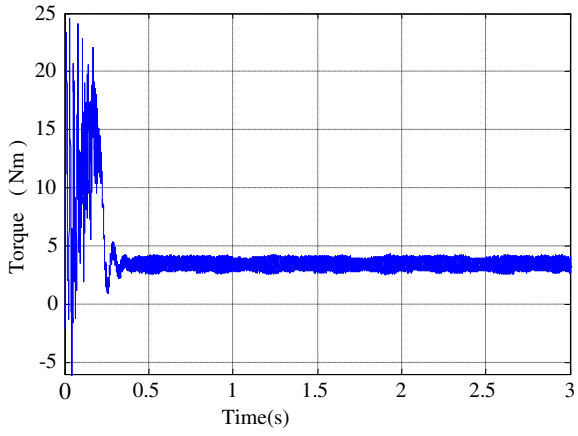

a)

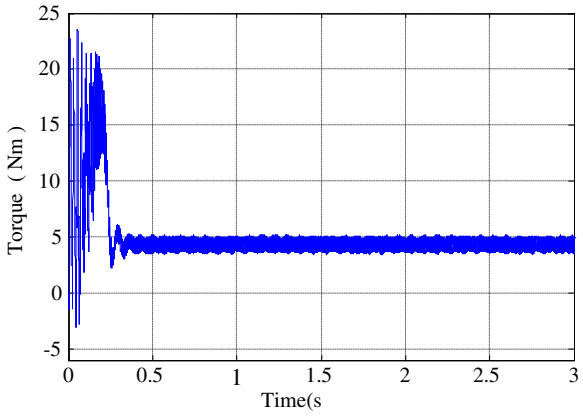

b)

Fig.6. Electromagnetic torque (40 % rated load load).
a) Two broken rotor bar b) Healthy Motor with oscillating torque.

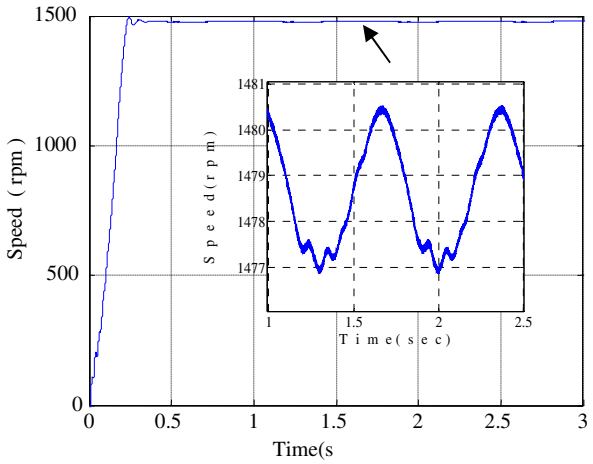

a)

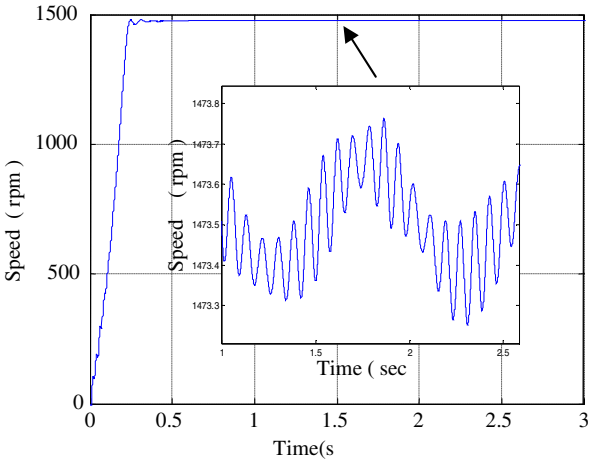

b)

Fig.7. Rotational Speed (40 % of rated load).
a) Two broken rotor bars b) Healthy Motor with oscillating torque.

IV. STATOR CURRENT ANALYSIS

The torque oscillation at a frequency (Fig. 8) generates a speed oscillation at this frequency whose amplitude depends on the inertia of the motor-load (Fig. 9).

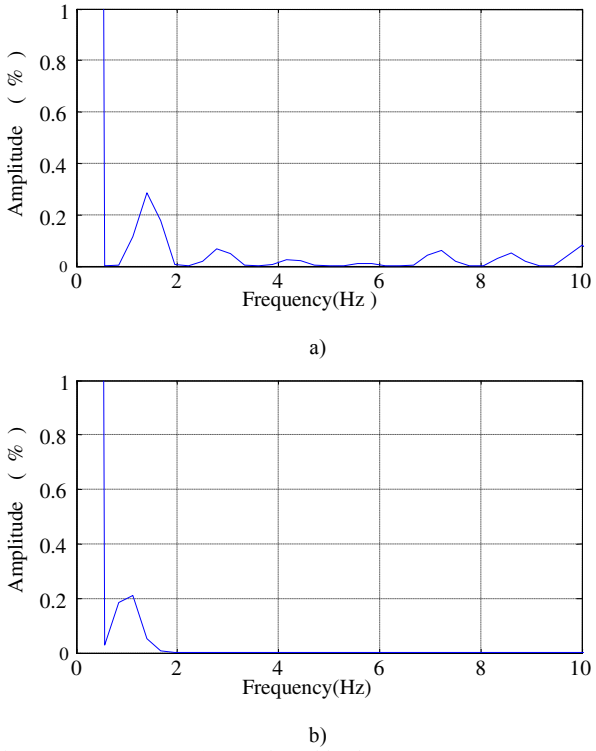

Fig.8. Torque spectrum (40 % of rated load)
a) Two broken rotor bars b) Healthy Motor with oscillating torque.

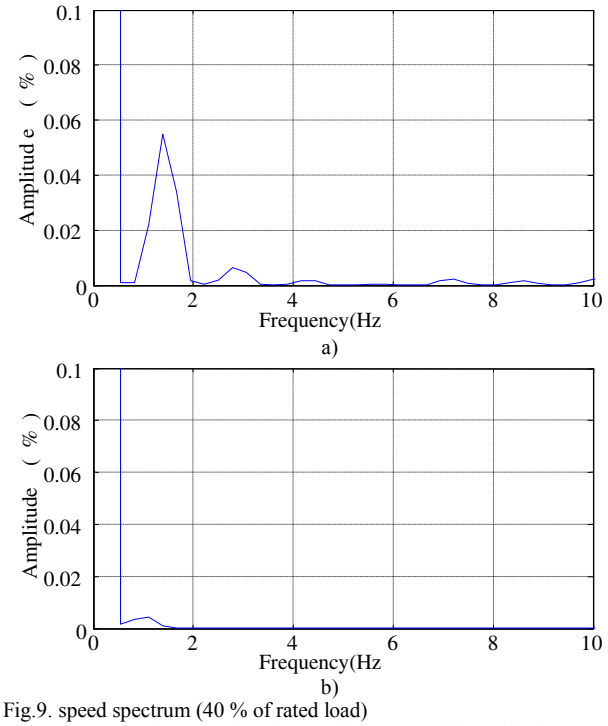

Fig.9. speed spectrum (40 % of rated load)
a) Two broken rotor bars b) Healthy Motor with oscillating torque.

Fig. 10.a, shows the current spectrum, sidebands at +2sf are produced by broken bars, fig. 10.b shows the stator current spectrum with sidebands at f_0=1 Hz produced by oscillating load which can be confused with broken bars. the broken rotor bars can't be distinguished from the oscillating load with MCSA.

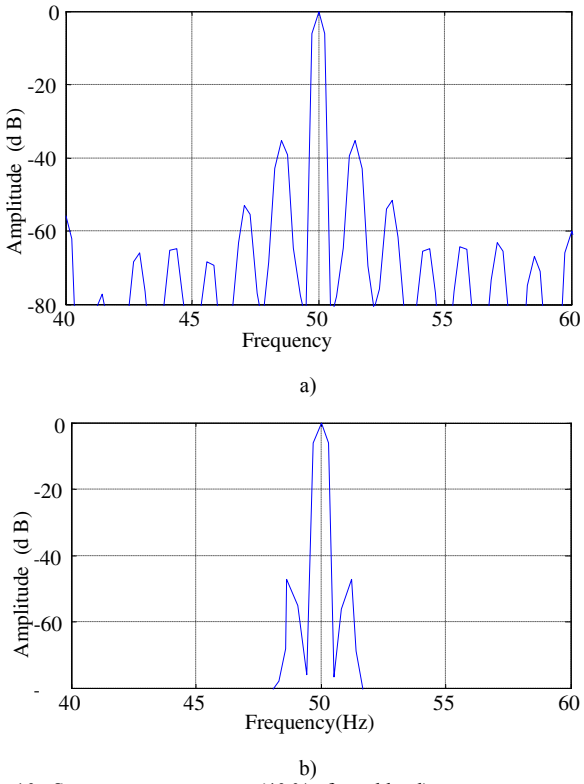

Fig.10. Stator current spectrum (40 % of rated load).
a) Two broken rotor bars b) Healthy Motor with oscillating torque.

V. ACTIVE AND REACTIVE POWER ANALYSIS

The normalized spectra of the instantaneous active and reactive power for the case of two broken bars (Figs. 11.a and b) show the appearance of a characteristic component directly at the frequency of speed oscillation, $f_0 = 2sf_s$, aside from the dc component. This characteristic component presents higher amplitude in the instantaneous reactive power spectrum with respect to the active power one. In the case of the load torque oscillation is exactly the opposite behavior as compared to the broken rotor bar case (Figs. 12.a and b).

The oscillating active power clearly reflect the effect of the oscillating load, the reactive power is practically negligible.

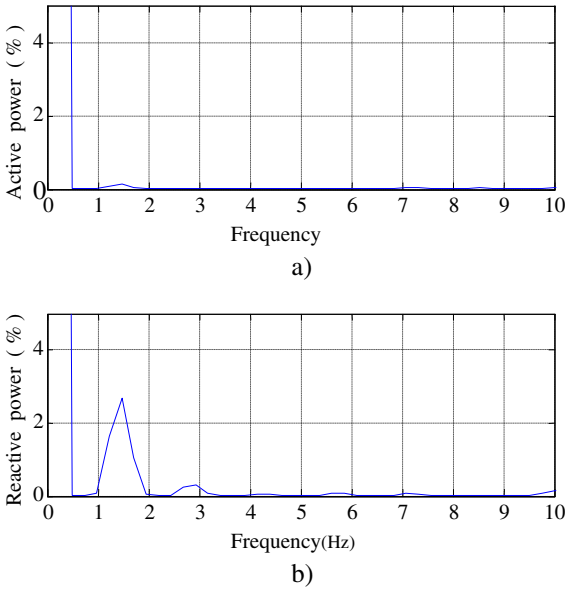

Fig. 11. Motor with two broken rotor bars (40 % of rated load)
(a) p(t) (b) q(t) spectrums.

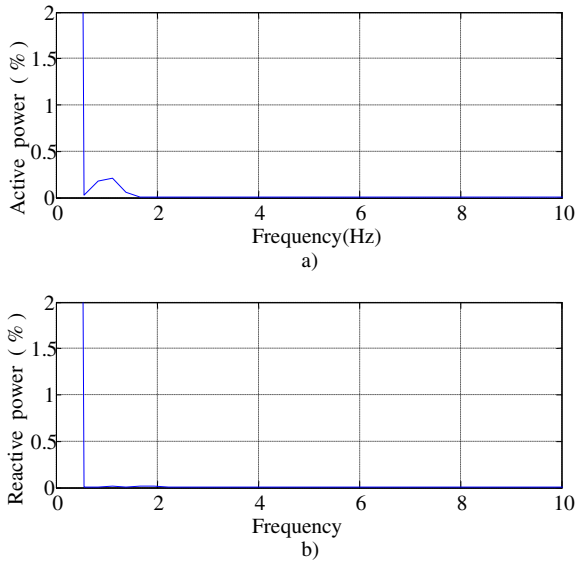

Fig. 12. Motor with oscillating torque (40 % of rated load)
(a) p(t) (b) q(t) Spectrums.

VI. EXPERIMENTAL RESULTS

In order to validate the simulation results, a special test bench was used. The test bench used in the exerimental investegation is avilable at the LGEB Biskra-Algeria (Fig. 13). The experimental test were carried out on three-phase induction machines (3 KW, 50-Hz, 4pole, 28 bars Y connected). The data acquisition was fixed to 10 seconds at a sampling frequency of 10 kHz through a D-Space 1104 board. A simulator torque which oscillates between two values according to time. The cycle frequency is adjustable from 0 to 200s and the cyclic ratio from 0% to 100%. Fig. 14.a shows the waveform of the torque used in the experiment. In this case, the load torque presents a sequence of harmonic components with a fundamental one at the frequency f_o=1 Hz (Fig 14.b). Their total effect can be considered as a superposition of a series of single frequency oscillating loads.

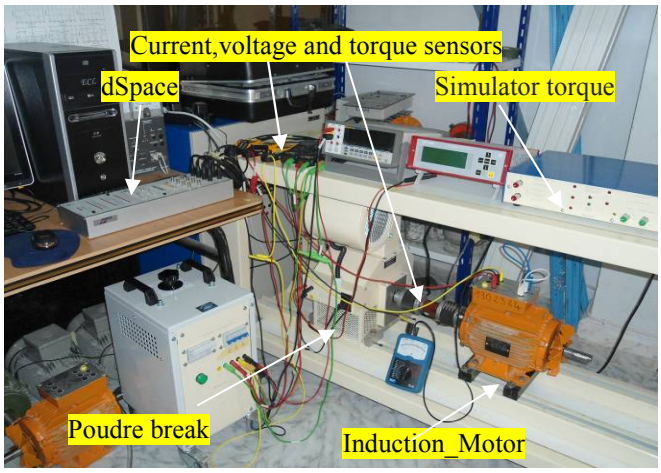

Fig. 13. Test-bed used for experimental analysis.

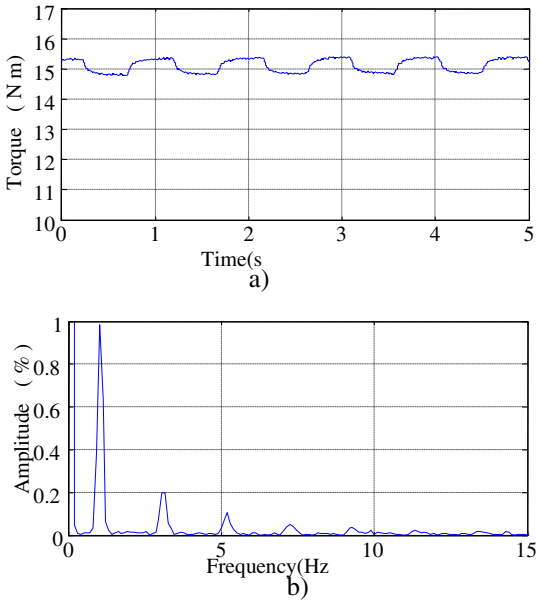

Fig. 14. The shaft torque
a) The waveforme b) Spectrum.

Fig. 15.a shows the current spectrum of the machine with two broken bars, Fig. 15.b shows the current spectrum of the healthy machine with load torque oscillation. Prominent sideband components appear at 51 Hz and 49 Hz, i.e., at 50 Hz (fundamental frequency) plus and minus 1 Hz (frequency of speed oscillation). A frequency component at 53 Hz, i.e., 50 Hz +2×1 Hz, was generated by the second harmonic of the pulsating torque, It is evident that the FFT analysis alone cannot distinguish between broken rotor bars and load oscillations.

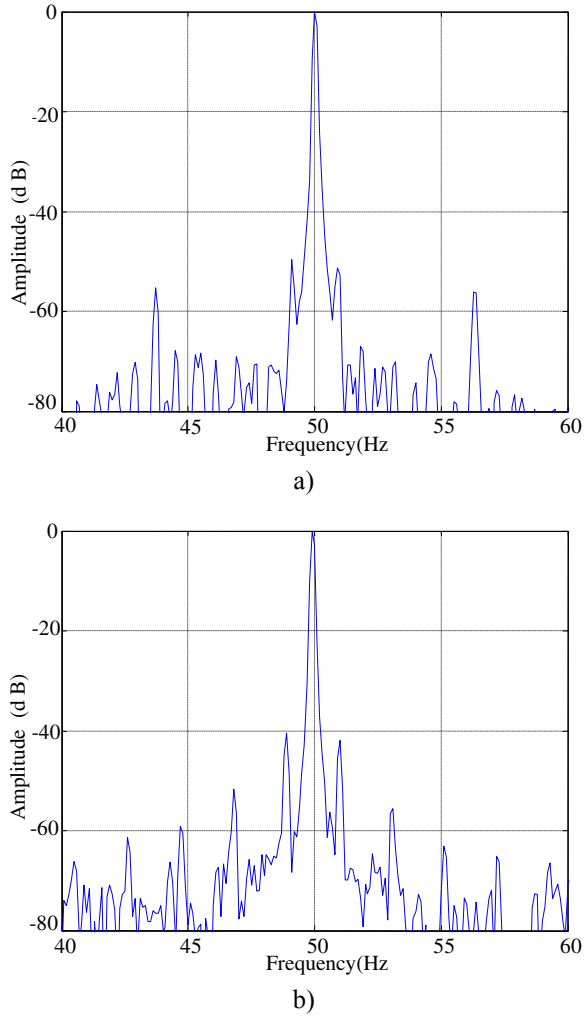

Fig.15. Stator current spectrum (40 % of rated load).
a) Two broken rotor bar b) Healthy Motor with oscillating torque.

The spectrum of the instantaneous active and reactive power in the case of motor with two broken bars is shown in Fig. 16.a and b, respectively. It can be appreciated that the instantaneous active power spectrum amplitude at 2s*f* is less than of the reactive power. In the case of the load torque oscillation, the normalized spectra of the instantaneous active and reactive power spectrum shows the appearance of sidebands at $n \times f_o$ (n=1,3,5,…..) due to the oscillating load. The magnitude of the instantaneous active power spectrum at f_o =1Hz which can be confused with the broken bar condition $2sf_s$ (s=0.01), is much greater than the reactive power one as shown in Figs.17.a and b, respectively.

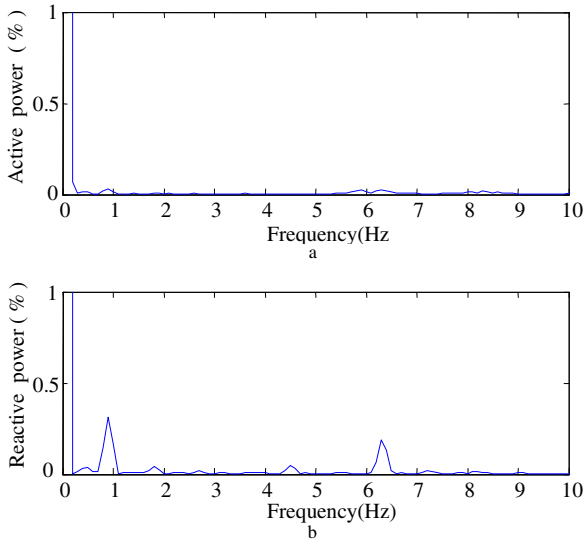

Fig. 16. Motor with two broken rotor bars (40 % of rated load).
(a) p(t) (b) q(*t*) spectrums.

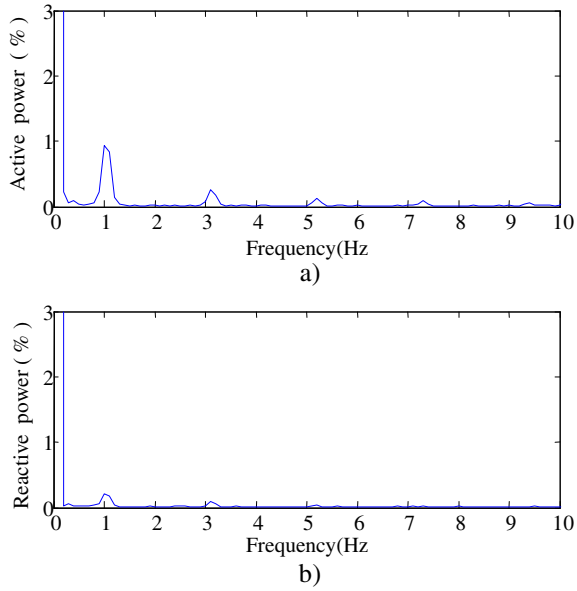

Fig. 17. Motor with an oscillating torque (40 % of rated load).
(a) p(t) (b) q(t) spectrums.

VII. CONCLUSION

This paper presents the circuit coupled finite element method used to modeling the Three-Phase Squirrel Cage Induction Motor. For this purpose, the time-stepping finite element method (TSFE) was proposed. The determination of magnetic flux density waveform, magnetic flux distribution was obtained. The perturbation in the air-gap magnetic field produced by broken bars results in a non-symetrical field. The flux densities have a symmetrical distribution in healthy state driven by oscillating load.

Discriminating rotor cage fault from oscillating load effects in Induction motors are considered. The computer simulations results shows that rotor fault conditions can be

separated from the abnormal mechanical load conditions by the combination of the active and reactive power signature analyses at frequencies of twice the slip frequency. The experimental results were confirmed that the proposed approach constitutes a useful tool for the study and diagnostics of induction motors.

VIII. APPENDIX

TABLE I
ELECTRICAL AND GEOMETRICAL CHARACTERISTICS OF SIMULATED INDUCTION MOTOR

characteristic	***value***
Rated power	*1.1 Kw*
Rated source voltage	*380 V*
Rated source frequency	*50 Hz*
Number of stator slots	*48*
Number of rotor slots	*28*
Outer diameter of stator core	*145 mm*
Inner diameter of stator core	*90.4 mm*
Outer diameter of rotor core	*89.8 mm*
Inner diameter of rotor core	*27.94 mm*
Air gap thickness	*0.3 mm*
Length of the stator and rotor core	*55 mm*

IX. ACKNOWLEDGMENT

The authors would like to thank Professor Champenois at the LAII laboratory, Poitiers, France, for his help.

X. REFERENCES

[1] G.B. Kliman, l. Stein, "Method of Current Signature Analysis", *Electric Machines and Power Systems*, vol. 20, pp. 463-474,1992.

[2] A. Bellini, F. Filippetti, G. Franceschini, C. Tassoni, and G. Kliman, "Quantitative evaluation of induction motor broken bars by means of electrical signature analysis ", *IEEE Trans. Industry Application*, vol. 37, pp. 1248–1255, Sept./Oct. 2001.

[3] R. R. Schoen, T. G. Habetler, "Effects of time-varying loads on rotor fault detection in induction machines", *IEEE Trans. Industry Application,* vol. 31, pp. 900–906, July/Aug. 1995.

[4] S. M. A. Cruz and A. J. M. Cardoso, "Rotor cage fault diagnosis in operating three-phase induction motors, under the presence of time-varying loads", presented at the Eur. Conf. Power Electronics Application, Graz, Austria, 2001.

[5] W. Long, T. G. Habetler, and R. G. Harley, "Separating load torque oscillation and rotor fault effects in stator current-based motor condition monitoring ", presented at the IEEE Int. Conf. Electrical Machines and Drives, San Antonio, USA, May 2005.

[6] K. Bacha, M. Gossa, H. Henao, and G. A. Capolino, "A time-frequency method for multiple fault detection in three-phase induction machines", presented at the IEEE Int. Symp. Diagnostics Electrical Machines, Power Electronics and Drives, Vienna, Austria, 2005.

[7] C. Kral, H. Kappeler, F. Pinker, G. Pascoli, "Discrimination of rotor faults and low frequency load torque modulations of squirrel cage I.M.by means of the Vienna monitoring method ", presented at the IEEE Power Electronics Specialists Conference, Recife, Brazil, June, 2005.

[8] G. Salles, F. Filippetti, C. Tassoni, G. Crellet, and G. Franceschini, "Monitoring of induction motor load by neural network techniques", *IEEE Trans. Power Electronics*, vol. 1, pp. 762–768, Jul. 2000.

[9] C. Concari, G. Franceschini and C. Tassoni, " Induction machine current space vector features to effectively discern and quantify rotor faults and external torque ripple ", *IET Electric Power Applications*, Vol. 6, pp. 310-32, 2012.

[10] G. R. Bossio, C.H. De Angelo, J. M. Bossio, C. M. Pezzani, and G. O. Garcia, " Separating Broken Rotor Bars and Load Oscillations on IM Fault Diagnosis Through the Instantaneous Active and Reactive Currents ", *IEEE Trans. Industrial Electronics*, vol.56, pp.4571-4580, 2009.

[11] M. Drif, A. J. Marques Cardoso, "Discriminating the Simultaneous Occurrence of Three-Phase Induction Motor Rotor Faults and Mechanical Load Oscillations by the Instantaneous Active and Reactive Power Media Signature ", *IEEE Trans. Industrial Electronics,* vol. 59, pp. 1630-1639, 2012.

[12] C.H. De Angelo, G.R. Bossio and G.O. Garcia, " Discriminating broken rotor bar from oscillating load effects using the instantaneous active and reactive powers", *IET Electric Power Applications*, Vol. 4, pp. 281-290, Jan. 2010.

[13] S. M. A. Cruz, "An Active–Reactive Power Method for the Diagnosis of Rotor Faults in Three-Phase Induction Motors Operating Under Time-Varying Load Conditions", *IEEE Trans. Energy Conversion* , vol. 27, pp. 71-84, 2012

[14] S. M. A. Cruz and A. J. M. Cardoso, "Rotor cage fault diagnosis in three-phase induction motors by the total instantaneous power spectral analysis," presented at the Industry Applications Society Annu. Meeting, Phoenix, USA, 1999.

[15] S. E. Zouzou, S. Khelif, N. Halem, M. Sahraoui, "Analysis of induction motor with broken rotor bars using finite element method ", presented at the 2nd international conference on electric power and energy conversion systems, Sharjah, UAE, 2011.

[16] T. H. Pham, P. F. Wendling, S. J. Salon, and H. Acikgoz, "Transient finite element analysis of an induction motor with external circuit connections and electromechanical coupling ", *IEEE Trans. Energy Conversion*, vol. 14, pp. 1407–1412, Dec. 1999.

XI. BIOGRAPHIES

Mabrouk Abd Elhamid was born in Biskra (Algeria) on 1985. He received the Engineer and "Magistère" in electrical engineering from university of Med Khider of Biskra, Algeria in 2009 and 2012 respectively. He is currently pursuing Ph.D degrees at Med Khider University, Algeria. His research interests include modeling and simulation of faulty electrical machines and intelligent systems application.

Salah Eddine Zouzou was born in Biskra, Algeria on 1963. He received the B.S degree from the "Ecole Nationale Polytechnique d'Alger", Algeria in 1987 and the M.S and Ph.D degrees from the "École Nationale Polytechnique de Grenoble" France, in 1988 and 1991 respectively. His fields of research interests deal with the design and condition monitoring of electrical machines. He has authored or co-authored more than 50 scientific papers in national and international conferences and journals. Prof. Zouzou is a Professor at the University of Biskra, Algeria and he is the director of the "Laboratoire de Génie Electrique de Biskra" since 2003.

Mohamed Sahraoui was born in Biskra, Algeria in 1978. He received the Engineer, "Magistère" and the Ph degrees in electrical engineering from the University of Med Khider of Biskra, Algeria in 2001, 2003 and 2010 respectively. He is interested in the modelling, condition monitoring and faults diagnosis of electrical machines.

Samia KHELIF was born in ourgla (Algeria) on 1983. She received the Engineer and "Magistère" in electrical engineering from university of Med Khider of Biskra, Algeria in 2008 and 2012 respectively. She is currently pursuing Ph.D degrees at Med Khider University, Algeria. Her research interests include monitoring and faults diagnosis of electrical machines.